Journal of Applied Polymer Science

# Ionic Nanocomposite Networks in Poly(styrene-*co*-methacrylic acid) Copolymers with Calcium Carbonate

**Celine Chevallier,[1,2,3] Yiping Ni,[1,2,3] Ruben Vera,[1,4] Frederic Becquart,[1,2,3] Mohamed Taha[1,2,3]**

[1]Université de Lyon, F-42023, Saint-Etienne, France

[2]CNRS, UMR 5223, Ingénierie des Matériaux Polymères, F-42023, Saint-Etienne, France

[3]Université de Saint-Etienne, Jean Monnet, F-42023, Saint-Etienne, France

[4]Université Lyon I, Centre de diffractométrie Henri Longchambon, 43 boulevard du 11 novembre 1918, 69622, Villeurbanne, France

Correspondence to: M. Taha (E-mail: Mohamed.Taha@univ-st-etienne.fr)

**ABSTRACT:** To create reversible supramolecular ionic networks, ionic cross-links were formed from acid pendant functions in poly(styrene-co-methacrylic acid) copolymers by the addition of calcium carbonate. The random dispersion of acid functions in the polystyrene chain is ensured by NMR analysis. The partial reaction of the calcium carbonate with the carboxylic acids is highlighted by a limewater test. The influence of methacrylic acid and calcium-carbonate contents on the formation of an ionic network has been studied through solubility tests. Two main effects were obtained: the exfoliation of the unreacted calcium carbonate characterized by TEM is due to ionic interactions at the surface of nanometric particles that form the first level of organization of the calcium carbonate. Another part of the calcium carbonate reacts with carboxylic acid and is detached from particles to form clusters as shown by x-ray analysis. Finally, by analyzing the dynamic rheological spectrum, the conclusion that the strength of the ionic bonds arises with the calcium content is made. The interest of such an approach with a wide range of observed phenomena in the material is a one-batch process to make thermoreversible nanocomposite networks. © 2012 Wiley Periodicals, Inc. J. Appl. Polym. Sci. 129: 404–414, 2013

**KEYWORDS:** supramolecular structures; nanostructured polymers; synthesis and processing; cross-linking; structure–property relations

Received 10 July 2012; accepted 23 October 2012; published online 16 November 2012
**DOI: 10.1002/app.38757**

## INTRODUCTION

The introduction of ionic groups as pendant groups in organic polymers often leads to the formation of a copolymer showing a two-phase behavior.[1–3] This is due to the specific organization of ion pairs in the material, explained by several models, resulting on the apparition of a peak in small angle x-ray analysis.[4–6] In the matrix, the ion pairs attract each other through electronic interactions related to the size of the ions and the partial covalent character of the ionic bond.[4] Under a critical ion content, which depends on the nature of the matrix and the ions, these interactions do not overcome the elastic forces of the chains. Over it, the ion pairs aggregate in the matrix and are called multiplets. Their size is limited by steric factors. Around these multiplets, the polymer chains sustain a reduction in their mobility because each ion pairs in a multiplet effectively anchor the polymer chains at the point to which they are attached. In these areas, no ionic material is observed since ion pairs very close to a multiplet tend to be incorporated therein. If the ion content increases, the distance between multiplets decreases, and over a critical ion content, areas of restricted mobility overlap. As this overlap occurs more frequently, relatively large continuous regions of restricted mobility are formed. When such a region is large enough to have its own $T_g$, it constitutes a cluster (50–100 Å) and exhibits a separated phase behavior. If the ion content increases further, the polymer changes from a matrix-dominant material (which does not contain ionic material) to a cluster-dominant one.[4,7] The structure created is then nanometric and supramolecular as Lehn defined it (dynamic, reversible, and non-covalent).[8,9]

Many studies focus on the dynamic rheological and mechanical properties of styrene-based ionic polymers.[7,10–17] Two maximums are seen in the plot of loss tangent vs. temperature in these ionic polymers. This indicates, as the models predicted it, that only two distinct morphological regions are present in these materials (as opposed to a wide range of morphologies). They correspond to the unclustered and the clustered materials. The loss tangent peaks widths are dependent on the ion

**Table I.** $CaCO_3$ Powder Size Distribution Results, Performed by Mastersizer 2000 on a Dry Powder

| Volume average diameter (μm) | Surface average diameter (μm) | Specific surface area($m^2$/g) | Span (10–90%)[a] | Uniformity[b] | $d$(0.1) (μm)[c] | $d$(0.5) (μm)[c] | $d$(0.9) (μm)[c] |
|---|---|---|---|---|---|---|---|
| 29.03 | 3.786 | 1.59 | 2.517 | 3.15 | 1.953 | 7.832 | 21.663 |

[a]It is the coefficient of variation and represents the width of the size distribution. [b]It represents a deviation from the median.
[c]They are particles' diameters. Respectively 10, 50, and 90 vol % of the particles have a smaller diameter than respectively $d$(0.1), $d$(0.5), and $d$(0.9).

content: the width of the first peak (corresponding to the matrix $T_g$) increases, whereas the second one decreases when increasing the ion content. The exact opposite is observed in the heights of the peaks: the height of the matrix decreases, whereas that of clusters increases, when increasing the ion content. Indeed, the peak area can be regarded as a measure of the volume fraction of the clustered or unclustered material.[7]

The storage modulus curve shows three plateaus: the first one at low temperature is the glassy plateau, the second is called the ionic plateau, and the third is the common rubbery plateau, at high temperatures.[4,7,11,12,17] Kim et al.[7] studied these behaviors in detail and concluded that the glassy modulus (measured in the first plateau) does not depend on the ion content of the matrix. However, the moduli of the ionic and rubbery plateaus increase with the ion content. Hird and Eisenberg[12] stated that the existence of the ionic plateau is due to the multiplets' role of cross-links in the matrix and proved that they remain stable over high temperature range (above the matrix $T_g$). So it is called "ionic" plateau since it is related to the degree of clustering. The global increase in the modulus with the ion content is explained by the multiplets' role as reinforcing filler particles by Hird and Eisenberg.[12] But Kim et al.[7] compared Young's modulus values calculated with the Guth equation considering the volume fraction of either multiplets or clusters as the volume fraction of filler particles and concluded that the clusters, and not the multiplets, have to be considered as a filler. In fact, this conclusion is in agreement with the Eisenberg et al. model,[4] which considers that over a critical ion content, only the clusters have to be taken in account in the matrix.

All these studies are about ionomers, using exclusively metallic salts with different kind of cations (Na, Ca, Cu, and so on).[18–20] The aim of this study is to use directly calcium carbonate as received with no further purification and to study both the exfoliation of the filler and the formation of ionic supramolecular structure in the copolymer. The combination of these two phenomena can lead to interesting properties of the material.

There are only a few studies in the literature about filled ionomers. Most of them treat the plasticizing and filling effects of functional organic salts.[21–27] Under a certain amount, the organic salts aggregate with the ionic groups. Thus, they introduce more free volume to the cluster regions without affecting the amount of the cluster regions. Over it, they form phase-separated domains and act as fillers. When the length of the organic chain attached to the salt is high enough, the free volume introduced in cluster regions is so big that no filling effect is observed.[21,26] Other studies present the possible interactions between nanoclays, such as montmorillonite or silica with ionomers. They observe that the nanocomposites exist in both the non-ionic matrix and in the ionic cluster, due to the polar groups at the surface of the particles.[28–31] Even if this field has been developed in the last years, most of the studies are about ionomeric rubber, and the ionic effect of the fillers is investigated only to achieve a better dispersion.[32–35] In the case of calcium carbonate, it is known that the presence of the acid functions along the copolymer chains permits a strong interaction with $CaCO_3$ particles and their exfoliation in the matrix.[36–39]

In this study, the calcium carbonate is used both for a nanofilling effect and the ionic sites formation by its partial reaction with the acid pendant functions in the main polymer chain, leading to important changes in the physical properties of the material. Contrary to the quoted works, the ionomer is not created and then filled, but this is a one-batch process: a part of the filler will interact with the methacrylic acid and form ionic cluster regions, and the other part will act as a filler in a polymer matrix, and the exfoliation of it will lead to a nanocomposite.

The research ionic cross-linking conditions lead us to investigate a larger domain than the one classically studied. Indeed, the ionizable functions content is here 20 mol % in the main chain, whereas the quoted works rarely overpass 10 mol %. The influence of the calcium-carbonate content introduced before the styrene and methacrylic acid even polymerized (from 12 mol % to 22 mol %) is examined.

## EXPERIMENTAL

### Chemicals

Precipitated calcium-carbonate $CaCO_3$ (CCP SOCAL® 31) was obtained from Solvay (Brussels, Belgium). Styrene (Sty), methacrylic acid (MAA), 2,2-azobis(2-methyl-propionitrile) (AIBN), and tetrahydrofuran (THF) were purchased from Sigma-Aldrich. Styrene was distilled before used. All the other reactants were used as received without further purification.

The $CaCO_3$ powder size distribution was obtained with a Mastersizer 2000 particle size analyzer from Malvern (dry way with high air flow, the measures were repeated twice on the same sample). The particle size measured is from 0.01 to 10,000 $\mu$m of diameter.

The powder size distribution is measured on the dry powder, before any experiment was performed. The results are summarized in Table I.

### Equipments

ULTRA TURRAX from IKA®, working at 11,000 rpm, was used to disperse calcium-carbonate particles in the neat monomer solution.

### Dynamic Mechanical Spectroscopy

***Molten state rheology.*** Dynamic mechanical spectroscopy measurements in the molten state were carried out with a strain-

Applied Polymer SCIENCE

**Table II.** Formulation of the Five Samples Studied

| Nomenclature | Sty (mol %) | MAA (mol %) | $CaCO_3$ (mol %) | Sty (wt %) | MAA (wt %) | $CaCO_3$ (wt %) |
|---|---|---|---|---|---|---|
| PS(0.0) | 80.0 | 20.0 | 0.0 | 82.9 | 17.1 | 0.0 |
| PS(0.7) | 70.0 | 17.5 | 12.5 | 72.6 | 15.0 | 12.5 |
| PS(0.8) | 68.6 | 17.1 | 14.3 | 71.1 | 14.7 | 14.2 |
| PS(1.2) | 64.0 | 16.0 | 20.0 | 66.3 | 13.7 | 19.9 |
| PS(1.4) | 62.2 | 15.6 | 22.2 | 64.5 | 13.3 | 22.1 |

controlled Rheometrics Scientific ARES system equipped with parallel plates' geometry of 25 mm diameter. The gap was fixed near 2 mm, and the strain was fixed at 0.5% at 220°C.

***Solid-state rheology.*** The rectangular bars (length 50 mm, width 10 mm, and thickness 2 mm) were prepared from the plates described below. Dynamic temperature sweep tests were chosen with strain amplitudes of 0.1% at 30°C to about 1% at 180°C to keep the measured torque at a sufficient level and to stay in the linear viscoelasticity domain of the material. The ramp temperature was 3°C $min^{-1}$ from 30 to 200°C with a fixed auto-tension at a constant frequency at 1.0 rad $s^{-1}$. The same Rheometrics Scientific ARES system was used, but the dynamic shear was applied using the rectangular torsion tool.

Transmission Electron Microscopy (TEM) observations were carried on a Hitachi H-800-3 electron microscope coupled with a numeric camera AMT XR40 Hamamatsu. Ultrathin sections (ca. 30 nm thick) were cut from the samples at room temperature and collected on copper grids. Pictures were analyzed with the free ImageJ software.

NMR analyses were performed with a Bruker Advance III 400 spectrometer operating at 400 MHz for $^{1}$H-NMR analyses and 100.25 MHz for $^{13}$C-NMR analyses. Samples were dissolved in a mixture of DMSO-$d^6$ and $CDCl_3$ (50/50 vol %) with trifluoroacetic acid (TFA) drops to break the ionic network. The analyses were performed in 10 mm diameter tubes with about 400 mg of polymer in 0.6 mL.

X-ray scatterings were done with a Bruker D8 Advance. The detector was a position sensitive detector VÅNTEC-1 "SUPER SPEED," and the focusing diameter fixed at 500 mm. The wavelength was 1.54 Å, and the x-ray ceramic tube was supplied with 33 kV and 45 mA. For the films analyses, 3° opening gap on the fix PSD was used.

### Sample Preparation

The MAA/Sty ([mol]/[mol]) and $CaCO_3$/MAA ([mol]/[mol]) ratios were set to study their effect on the final properties of the material. AIBN is added to the mixture at 0.5 mol % of the monomers.

To confirm the methacrylic acid neutralization, it was mixed with the calcium carbonate using ULTRA TURRAX under an argon flow at 11,000 rpm for 4 min at room temperature. The gas released was submitted to the limewater test confirming the formation of carbon dioxide. This shows that the carbonic acid formed from the calcium-carbonate reaction with methacrylic acid was in equilibrium with carbon dioxide and water.

Before the polymerization starts, styrene and AIBN were added to the reactive medium. Thus, the initial mixture was composed of unreacted methacrylic acid, unreacted calcium carbonate, calcium methacrylate, water, styrene, and AIBN.

### Sample Preparation for Solubility Tests

To achieve the tetrahydrofuran solubility tests and the NMR analysis, 5 mL of the mixture was poured into a tube in a 70°C silicone oil bath for 7 h. The copolymer is put in a glass pot with 10 mL of THF for 48 h before performing the solubility test. The solution turned turbid because of the insoluble calcium carbonate.

### Sample Preparation for Mechanical Tests

To make the copolymer plates, around 30 g of the same mixture was transferred in a 250 mL glass reactor with an anchor for mechanical stirring, at 150 rpm. The reactor was placed in a silicon oil bath for pre-polymerization at 70°C for 40–60 min until the blend becomes viscous enough, based on a chosen torque value corresponding to a sufficient viscosity level. The reactive and viscous system was finally poured into a mold (2×100×100 mm) and pressed under 200 bars at 70°C for 7 h.

These plates were realized for only four filled calcium-carbonate samples. The MAA/Sty ([mol]/[mol]) ratio was settled at 0.25, and the $CaCO_3$/MAA ([mol]/[mol]) ratio varied from 0.7 to 1.4. The samples were named as following: PS ($CaCO_3$/MAA ratio). The four samples are PS (0.7), PS (0.8), PS (1.2), and PS (1.4). A fifth sample was analyzed, a non-filled copolymer with the MAA/Sty ratio fixed at 0.25, named PS(0.0). The formulations of these copolymers are resumed in Table II.

A size exclusion chromatography analysis was carried out on the non-filled sample (PS[0.0]). It was conducted using a system (515 Waters) equipped with a triple detector consisting of a refractive index detector (Waters 2414), a Wyatt MiniDawn Treos low-angle light-scattering detector, and a Wyatt Visco star viscometer. Two columns HR 0.5 and HR 3 from Waters were used. Molar masses were determined by DDL with index of refraction increment d*n*/d*c* values calculated for each sample using the Wyatt Astra 5.3.4 software. THF is used as mobil phase (Biosolve, GPC grade) at a flow rate of 1 mL $min^{-1}$, and the sample concentration was 3 mg $mL^{-1}$. The injection volume was 100 $\mu$L. The number average molar mass was 310,800 g/mol, the weight average molar mass was 2,064,000 g/mol, and hence, the polydispersity was found equal to 6.64.

## RESULTS AND DISCUSSION

### Copolymers Microstructures

In order to study the tacticity and the distribution of monomers in the copolymer chains, $^{13}$C-NMR was performed.

$^{13}$C-NMR spectra allow the attribution of some peaks to monomer triads centered on the styrene and on the methacrylic acid monomers. A wide range of Sty/MAA ([mol]/[mol]) ratios is needed, and the copolymers made are resumed in Table III.

The entire spectrum of one of the copolymer (50S50MAA) is represented in Figure 1.

**Table III.** Formulation of the Copolymers Created for NMR Analysis

| Nomenclature | Sty (mol %) | MAA (mol %) | $CaCO_3$ (mol %) |
|---|---|---|---|
| 100S0MAA | 85.7 | 0 | 14.3 |
| 95S5MAA | 81.4 | 4.3 | 14.3 |
| PS(0.8) | 68.6 | 17.1 | 14.3 |
| 50S50MAA | 42.8 | 42.8 | 14.3 |
| 20S80MAA | 17.1 | 68.6 | 14.3 |
| 5S95MAA | 4.3 | 81.4 | 14.3 |

The indexation of the peaks in this spectra and the attribution of the triads shown in Figures 2 and 3 have been done from the Brar and Hekmatayar study.[40] They indexed the M**M**M (MAA/**MAA**/MAA), M**M**S (MAA/**MAA**/Sty), and S**M**S (Sty/**MAA**/Sty) triads from the carbonyl resonances around 180 ppm (Figure 2). The S**S**S (Styr/Sty/Sty), S**S**M (Sty/Sty/MAA), and M**S**M (MAA/Sty/MAA) triads, centered on a styrene unit, are identified from the resonances around 145 ppm corresponding to tertiary carbon (Figure 3).

From the zoom of the $^{13}$C-NMR spectrum around $\delta$180 ppm (Figure 2), the three triad peaks are separately observed: the S**M**S triad appears between 177 and 178 ppm, and both the M**M**S and M**M**M triads, respectively, between 178 and 179.5 ppm and between 179.5 and 181 ppm. The spectrum of PS(0.8) shows no M**M**M triads: the methacrylic acid units are well-dispersed in the chains, and its distribution is atactic. In Figure 3, the observation is focused on the styrene $C_1$ carbon resonance; the triads are attributed as follow: S**S**S between 144 and 146.5 ppm, S**S**M between 146.5 and 147.5 ppm, and M**S**M between 147.5 and 149 ppm. The copolymer PS(0.8) shows only the S**S**S triads. The structure of the comonomers in the polymer chain is predominantly composed of styrene (due in part to the 80 mol %), and methacrylic acid is well dispersed.

In conclusion, a random distribution of the MAA units in the PS chain is now considered and proved.

**Solubility of PS/MAA/CaCO3 Samples**

The MAA/Sty ([mol]/[mol]) and $CaCO_3$/MAA ([mol]/[mol]) ratios, which allow the ionic supramolecular network formation, were found from solubility tests of the polymer matrix in THF.

The results of the solubility tests in tetrahydrofuran (THF) are summarized in Figure 4. The result is binary (soluble when the THF solution turned slightly turbid or swelling when the initial shape of the polymer sample was still recognizable in the tube; more details are given in experimental) and depends on the MAA/Sty and $CaCO_3$/MAA ratios.

**Influence of the MAA/Sty ([mol]/[mol]) Ratio.** The solubility tests prove that the acid monomer proportion in the main chain plays a role: when it is high enough (for a $CaCO_3$/MAA ([mol]/[mol]) ratio fixed), the samples become insoluble; thus, a network is assumed to be created. However, when the MAA/Sty ([mol]/[mol]) ratio is <0.2, the samples turn soluble. The concentration of acid functions in the copolymer is too low, and apparently, no network can be formed.

**Influence of the CaCO3/MAA ([mol]/[mol]) Ratio.** The MAA/Sty ([mol]/[mol]) ratio is fixed (represented by a horizontal line in Figure 4), and so the $CaCO_3$/MAA ([mol]/[mol]) content effect, and by extension the calcium content effect, can be investigated.

For low calcium content, the samples are soluble, and they swell when the $CaCO_3$/MAA ([mol]/[mol]) ratio increases. The limit between solubility and swelling is dependent on the MAA/Sty ([mol]/[mol]); that is to say that for each MAA/Sty ([mol]/[mol]) ratio, there is a critical calcium content from which the

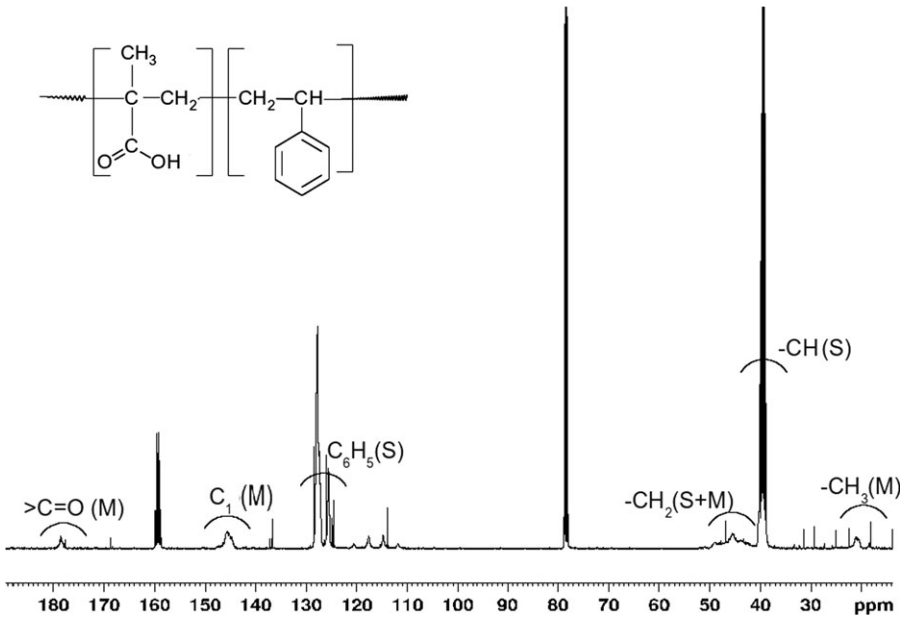


**Figure 1.** $^{13}$C-NRM spectra of the 50S50MAA copolymer in DMSO-$d_6$ and $CDCl_3$ (50/50 vol %) with TFA at 20°C.

Applied Polymer SCIENCE

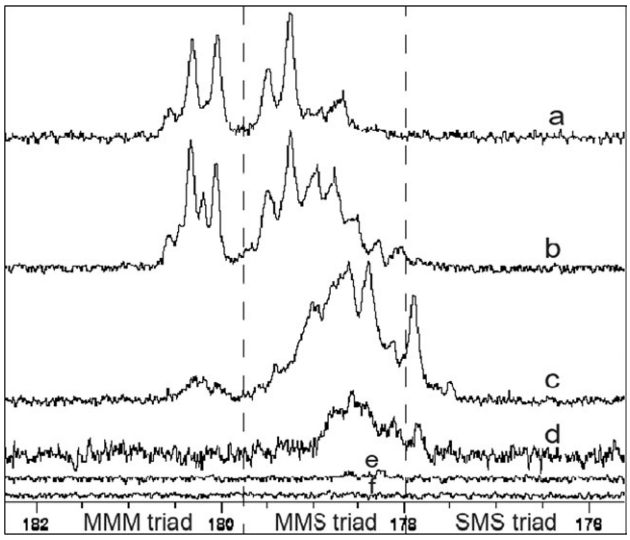


**Figure 2.** Triads attributions from the carbonyl carbon resonance by $^{13}$C-NMR in DMSO-$d_6$ and $CDCl_3$ (50/50 vol %) with TFA at 20°C: (a) 5S95MAA; (b) 20S80MAA; (c) 50S50MAA; (d) PS (0.8); (e) 95S5MAA; and (f) 100S0MAA.

copolymer becomes insoluble in THF. When the calcium-carbonate content is not high enough, no network was formed.

To conclude, both acid functions and calcium-carbonate content have a great influence on the formation of a network in the material. To find out what kind of network was formed in the matrix, the calcium-carbonate dispersion is examined.

### Calcium Carbonate Dispersion

The MAA/Sty ([mol]/[mol]) was kept constant and equal to 0.25 to observe the calcium-carbonate dispersion in the polymer matrix with TEM images analysis. The powder size distribution

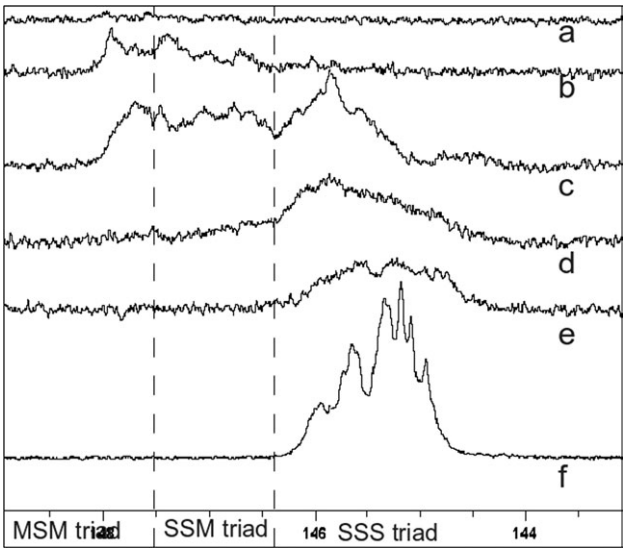


**Figure 3.** Triads attributions from the tertiary C1 carbon resonance by $^{13}$C-NMR in DMSO-$d_6$ and $CDCl_3$ (50/50 vol %) with TFA at 20°C: (a) 5S95MAA; (b) 20S80MAA; (c) 50S50MAA; (d) PS (0.8); (e) 95S5MAA; and (f) 100S0MAA.

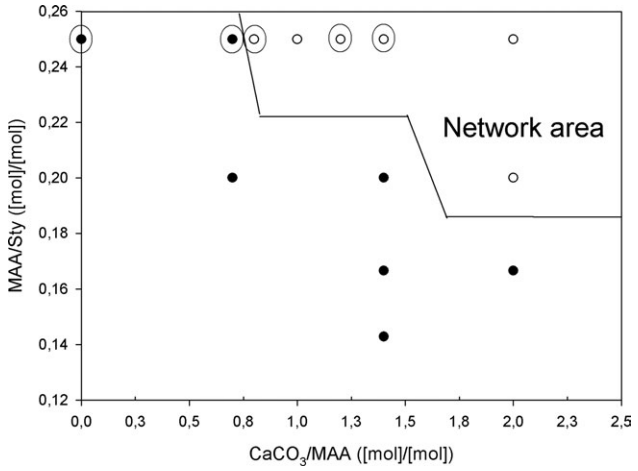


**Figure 4.** Solubility diagram of poly(styrene-co-methacrylic acid) with $CaCO_3$ in THF in 48 h at room temperature for different $CaCO_3$/MAA and MAA/styrene ratios: ● Soluble, ○ Swelling.

of $CaCO_3$ is compared to the TEM micrographs analyzed with the ImageJ software.

After preparing plates as described previously, TEM pictures have been taken at four magnitudes: 7000×, 10,000×, 50,000×, and 80,000×, in two different locations in each sample. Figure 5 presents only the 7000× magnitude of one typical location.

**TEM Pictures Analysis.** To quantify the observations, an analyzing picture software is used: ImageJ. This free software gives the average size (of the particle agglomerates, in nm$^2$), the area fraction (fraction of area occupied by particles, in nm$^2$), and the perimeter (of the agglomerates contained in the picture, in nm). From the average size and to compare these results with those obtained from the size distribution powder analysis, an average diameter is calculated, considering the agglomerates' shape as circles. Table IV summarizes the results from ImageJ analysis on the pictures taken at the lowest magnitude (7000×), to have the most general view of the sample.

The average size, the average diameter, and the perimeter of the agglomerates increase when the $CaCO_3$/MAA ratio decreases. The area fraction decreases with the particle content. As expected, the more particles there are in the matrix, the higher is the area occupied by them. But it is surprising to see that when the calcium-carbonate content arises, the dispersion seems better (i.e. the average size and diameter of the particles are smaller), especially between the two more added and the other two (PS [1.4] and PS [1.2] versus PS [0.8] and PS [0.7]). The particles agglomerate only at low content.

**Comparison Between Agglomerates Seen in TEM Pictures and Initial Powder Size Distribution.** In Table I, the volume average diameter measured on the dried powder is 29.03 $\mu$m, but in fact, as the uniformity is high (3.15), the diameters cover a large range. However, only 10% of the particles have a diameter $<$1.953 $\mu$m (d[0.1]), and none of them were measured with a diameter $<$0.138 $\mu$m, i.e. 138 nm. From the TEM micrographs analysis (in Table IV), the average diameters measured are below this value: from 30 to 100 nm. But, within the

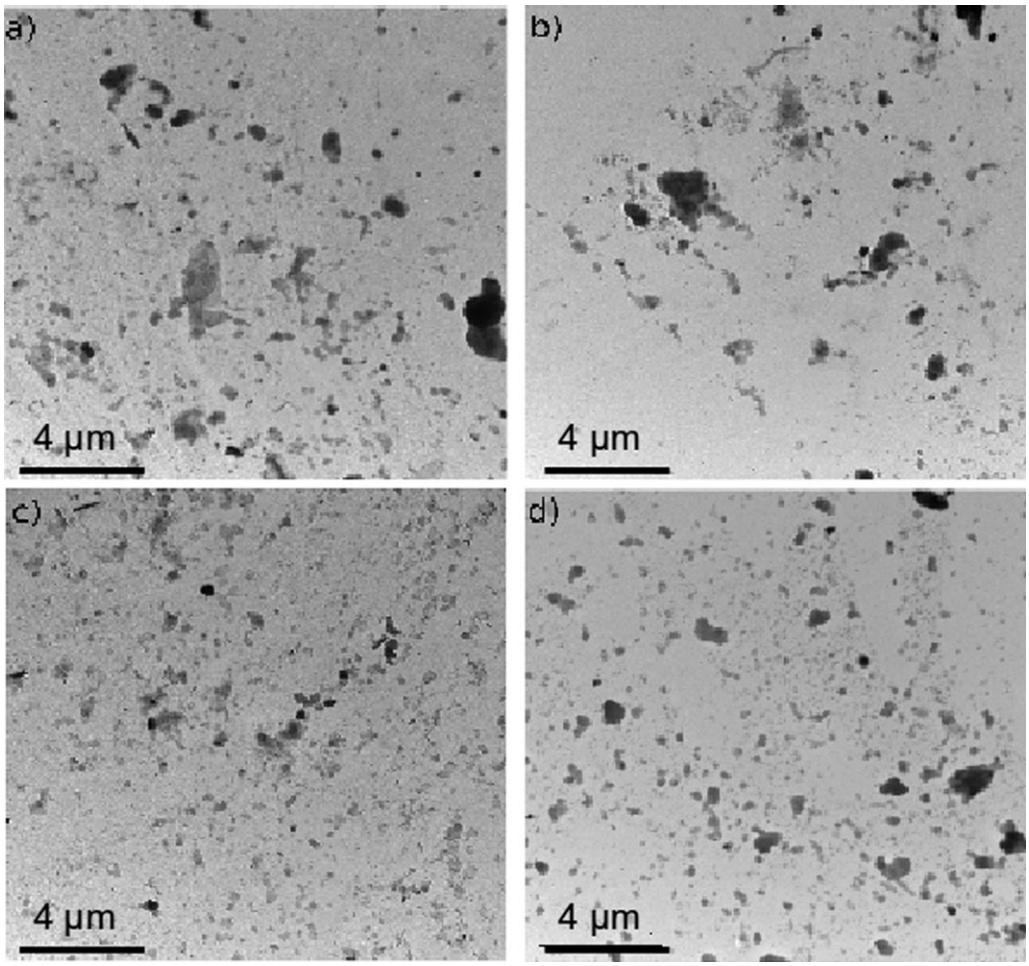


**Figure 5.** TEM pictures of (a) PS(1.4); (b) PS(1.2); (c) PS(0.8); (d) PS(0.7).

measurement error, Figure 6 shows that some particles remain at the same size before and after the polymerization. Even if some particles remain the same, most of them present an average size divided by three. The mechanical mixing using the ULTRA TURRAX and the strong interactions with the methacrylic acid manage to disperse very well the calcium carbonate in the copolymer matrix.

To conclude, the big agglomerates of initial calcium carbonate have been exfoliated, as shown by the drastic decrease in the average size. This phenomenon is due to the acid functions in polymer chains bonded at the surface of the agglomerates via ionic interactions.[36–39] This is the first organization of the calcium carbonate.

**Table IV.** Summary of ImageJ Analysis (on 7000× TEM pictures) Results

| | Average size ($nm^2$) | Average diameter (nm) | Area fraction ($nm^2$) | Perimeter (nm) |
|---|---|---|---|---|
| PS(1.4) | 3922 | 35.3 | 18.3 | 160 |
| PS(1.2) | 4980 | 39.8 | 12.8 | 182 |
| PS(0.8) | 10848 | 58.8 | 11.0 | 313 |
| PS(0.7) | 33967 | 104.0 | 8.9 | 541 |

To find if another organization is present in the matrix and could be partly responsible of the solubility tests' results, x-ray analysis has been performed.

### Clusters

X-ray analysis was performed to prove the ionic nanometric structure from the observation of the "ionic peak."[4–6] The analyses were performed on films thinner than 100 nm instead of

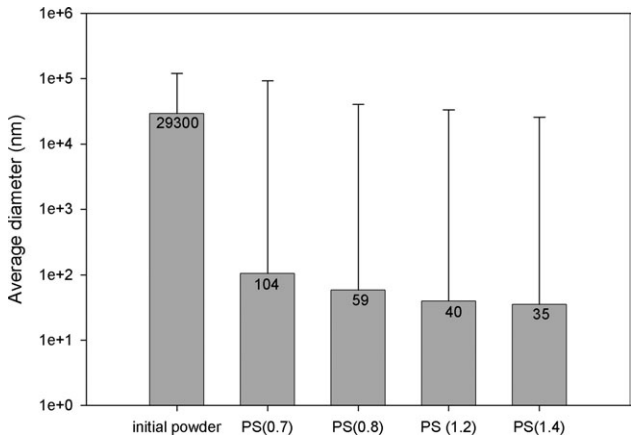


**Figure 6.** Average diameters of $CaCO_3$ particles with measurement errors.

powder samples. The $2\theta$ range is from 2.5 to 5.5°, centered on the ionic peak. The results are presented in Figure 7.

All the samples show a peak in this $2\theta$ range: for PS (0.8), PS (1.2), and PS (1.4), the peak starts at 3.7° and finish at 3.9°, which corresponds at a Bragg distance between 22.6 and 23.9 Å. This result corresponds to the intermultiplet distance of Eisenberg's model.[4] For the PS (1.2) and the PS (1.4), the ionic peak does not seem as evident as the other samples. The fact that these two samples are more filled than the others can explain this observation: the big calcium-carbonate aggregates can hinder the cluster formation by inserting in the cluster phase.[28–31]

The PS (0.7) peak extends from 3.8 to 4.3° $2\theta$ range, i.e. 20.5 to 23.2 Å. This result is still in the range given by Eisenberg et al., and the slight diminution of the intermultiplet distance can be explained as follows: the PS (0.7) is the copolymer that contains the less calcium, and it is assumed that it contains the less ionic pairs. The region of restricted mobility surrounding multiplets can be thinner than that of the others copolymers, and so, the multiplets can be closer to one another.

In conclusion, the ionic peak establishes that multiplets are created and that a cluster organization is present in the material. This is the second organization of the calcium in the matrix.

If the network in the material was totally ionic, it should be formed when the $CaCO_3$/MAA ([mol]/[mol]) ratio is settled to 0.5, and the samples should have been swelling from this value in the solubility tests. But the lowest value observed to form a network is 0.8. This fact means that, as shown with TEM, the calcium carbonate was not entirely dissociated by the acid functions. There is equilibrium between solid calcium carbonate and calcium cation in the cluster phase, and increasing calcium or acid content disturbs this equilibrium. The analysis proved that two kinds of interactions and structures are present in the material. To find out in which way they may have influenced the physical properties of the material, dynamic rheological analysis has been performed.

## Dynamic Rheology Analysis

The physical properties of the material were investigated through dynamic rheological analysis in the melt and the solid state.

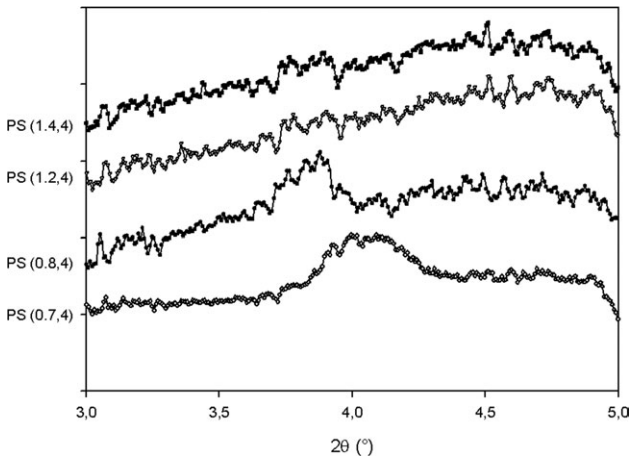


**Figure 7.** X-ray scattering patterns centered on the ionic peak of the ionic copolymers films.

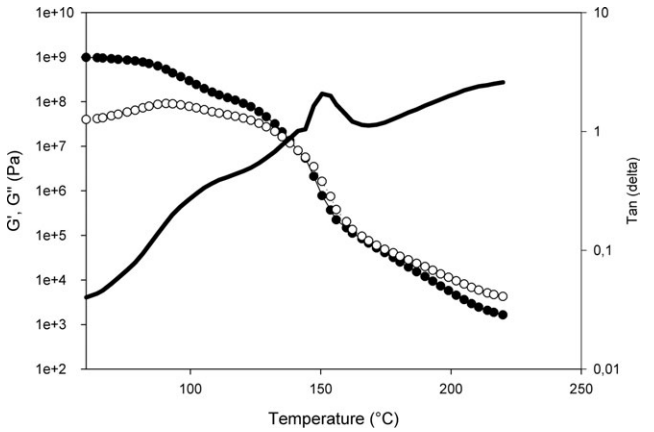


**Figure 8.** Rheological analysis of PS(0.7) ($CaCO_3$/MAA = 0.7), strain = 0.01–5%; frequency = 1 rad/s; ramp rate = 3°C/min; ● $G'$ (Pa), ○ $G''$ (Pa), – $\tan(\delta)$.

As all the samples present the same type of rheological curve, only one of them is represented here (Figure 8). Five areas can be examined: at low temperatures is the glassy plateau, followed by a little decrease in modulus when the first transition temperature is overpassed. A second plateau appears, called the "ionic" plateau, even if several parameters have to be taken in account (hydrogen bonding and filler effect). A second transition occurs, and finally, there is the viscous flow zone.

## Solid-State Analysis

***Study of the glass temperatures.*** The first maximum in the $G''$ curve of the PS(0.0) shows a smaller amplitude than the other samples (Figure 9). However, the second drops are similar: the modulus values lose about $10^{+3}$ Pa (from $10^{+8}$ Pa to $10^{+6}$ Pa) whatever the sample.

The values of transition temperatures are summarized in Figure 10. $T_{\alpha 1}$ is the temperature picked when the loss modulus $G''$ reaches a maximum around 100°C, and $T_{\alpha 2}$ corresponds to

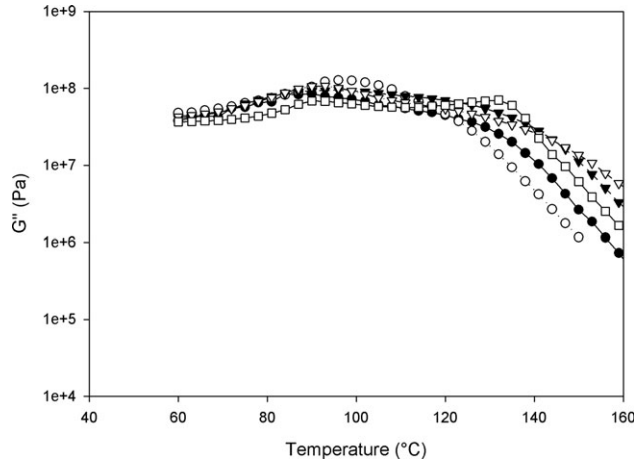


**Figure 9.** Storage modulus $G''$ comparison in the region of the glassy plateau: PS(x) ($CaCO_3$/MAA = x); □ PS (0.0), ● PS (0.7), ○ PS (0.8),▼ PS (1.2), ▽ PS (1.4).

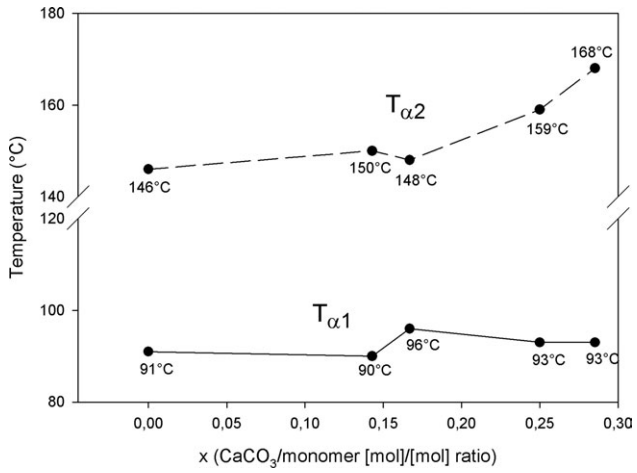


**Figure 10.** Evolution of the transition temperatures with the $CaCO_3$/monomers ratios.

tan($\delta$) curve's maximum around 150°C, depending on the samples and their formulation.

From the Fox equation[41] and the ratio MAA/Sty ([mol]/[mol]) settled to 0.25, the transition temperature observed should be equal to 117°C, and a simple barycenter relation gives a glass temperature equal to 122°C. Yet, two transitions are observed and, if the first one does not seem to evolve with the calcium content, the second one obviously does (Figure 10).

Hird and Eisenberg[12] are one of the first authors who explained the presence of two glass temperatures. They attributed the peak at the lowest temperature to the matrix $T_\alpha$, i.e., the ion-poor phase, and the second peak to the cluster $T_\alpha$, i.e., the ion-rich phase. According to that, it is normal that the $T_{\alpha 1}$ remains stable whatever the sample (Figure 10). Its value corresponds to the glass temperature of the non-ionic poly(styrene-co-methacrylic acid). This $T_\alpha$ increases about 3°C when the calcium content arises. This may be due to the filling effect of the calcium carbonate.

Every sample shows a second $T_\alpha$, even the non-ionic one. This cannot be attributed to an ionic effect but to the creation of a hydrogen-bonding network between non-ionic acid functions. In the added samples, this network is still there, at best the same but more probably hindered by the filling and ionic effects. Indeed, as the proportion of acid functions in the main chain does not evolve, the $T_{\alpha 2}$ should not evolve if it is only induced by H-bonding. However, it increases by 20°C and taking in account only the filling effect cannot explain such a result. So, as many authors did before,[7,10–17] the higher $T_\alpha$ of the added samples is attributed to the cluster phase and considered to evolve because of the ionic interactions (in the cluster phase and around the calcium-carbonate particles). The variation in temperatures is especially seen in the case of the PS (1.2) and the PS (1.4), and it can be related to the better filler dispersion observed in these two samples: the interactions between the acid functions and the calcium carbonate seemed more efficient in these cases. This temperature can be assumed as representative of the strength with which the ion pairs are held in a multiplet because it is the temperature from which they are able to migrate from one multiplet to another.[12] On this basis, the networks in the PS(0.7) and PS(0.8) show weaker ionic interactions in the multiplets than the ones formed in PS(1.2) and PS(1.4).

***Glassy plateau examination.*** At low temperatures, the storage modulus $G''$ is in the same range of values for each samples ($10^{+9}$ Pa) in agreement with the analysis of Kim et al.[7] about the glassy state. The storage modulus measured with a constant frequency reflects the chain mobility in the polymer. As expected, under the glass temperature of the matrix, the chains' mobility is of very short range and is not affected by the presence of multiplets (or fillers).

***Ionic plateau examination.*** The intermediate region, in which the modulus slightly decreases with the increase in temperature, is the ionic plateau. It is assumed to be existing since the multiplets form cross-links[12] and found to evolve with the ion content, for a range of 2–11 mol % of ion material.[7] After the matrix glass transition, the polymer chains are able to move, but these cross-links prevent the chains' mobility, resulting in the ionic plateau in the modulus curves (Figure 11). The ionic cross-links remain stable until the temperature becomes high enough to allow the ion pairs to migrate between multiplets. These migrations yield to a detectable drop in the modulus, which corresponds to the cluster glass transition, as discussed above. This plateau is independent of the calcium content (for this range of ion content, i.e. 20–40 mol %), as the modulus and the temperatures at which it starts and ends do not evolve linearly with it.

The un-added copolymer presents an intermediate plateau too due, as explained previously, to the H-bonding network formation.

## Melt State Rheology

***Viscous flow examination.*** The viscous flow zone is examined for each sample. When the $G'$ or $G''$ modulus are focused, a gentle decrease in their slopes is observed. As the cluster glass transition is overpassed, the multiplets are still present in the

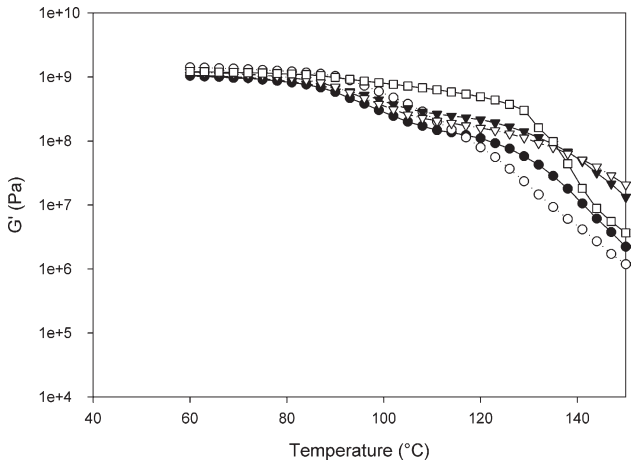


**Figure 11.** Storage modulus $G'$ comparison in the region of the ionic plateau PS(x) ($CaCO_3$/MAA = x); □ PS (0.0), ● PS (0.7), ○ PS (0.8), ▼ PS (1.2), ▽ PS (1.4).

matrix, as proved by SAXS (small-angle x-ray scattering) analysis.[12] As the $T_\alpha$ of a polymer means a mobility of its chains, the $T_\alpha$ of the clustered region represents the ability of the ion pairs inside the clusters to migrate from one multiplet to another.[12] When the temperature increases, these moves are multiplying, causing this slope in the viscous flow zone.

Tan($\delta$) values (Figure 12) show an interesting progression with the calcium-carbonate content. At high temperatures, an increase is observed in the tan($\delta$) values when the ratio $CaCO_3$/MAA ([mol]/[mol]) decreases. This enhancement of tan($\delta$) corresponds to a more viscous than elastic material. So the more the copolymer is added, the less viscous it is in the melt state. This behavior is related to the effective cross-link density in the network: if there is a lot of ionic material in the same matrix (MAA/Sty ([mol]/[mol]) = 0.25), the elastic nature is preponderant.

The PS(0.0) copolymer shows a very different evolution of tan($\delta$), in relation to the different type of network present in the matrix (H-bonding network). The tan($\delta$) values increase very quickly in comparison with the other samples.

***G′ and G″ cross-over study.*** The intersection of $G'$ and $G''$ modulus at high temperatures evolves when the calcium-carbonate content changes. Figure 13 shows the comparison of the cross-over temperatures, and the temperatures at which they take place are summarized in Table V.

The cross-over zone is very large and begins at the same temperature than the $T_{\alpha 2}$. To compare the cross-over values, the temperatures in Table V were chosen after $G''$ overpassed $G'$ and for a tan($\delta$) value equal to 1.5.

Only the PS (1.4) does not present a cross-over temperature: it may take place at a temperature higher than 220°C, from which the cooling started. By this assumption, the temperature of the crossing-over appears to increase with the calcium content and so the density of effective ionic cross-links. After the temperature of crossing-over is overpassed, the supramolecular interactions are not strong enough to sustain cross-linked material

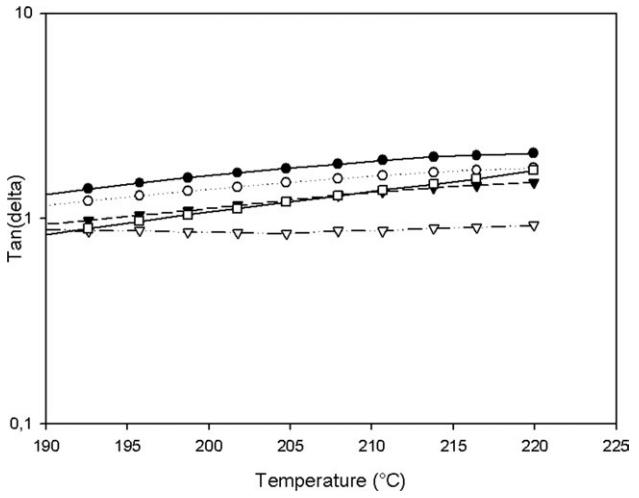


**Figure 12.** Tan($\delta$) in the melt state for each copolymer PS(x) ($CaCO_3$/MAA = x); □ PS (0.0), ● PS (0.7), ○ PS (0.8),▼ PS (1.2), ▽ PS (1.4).

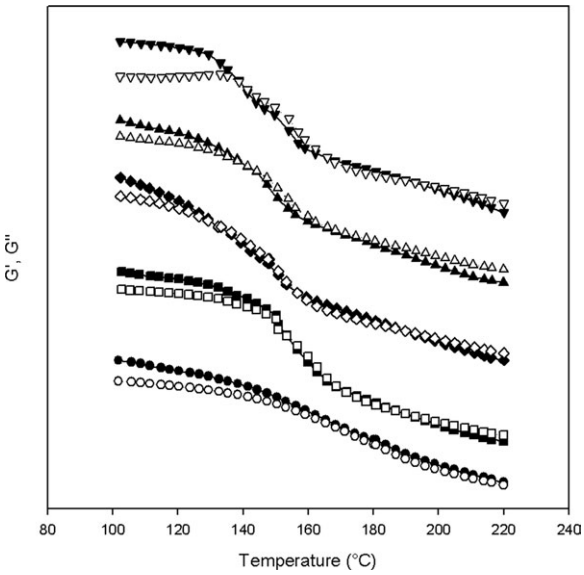


**Figure 13.** Comparison of $G'$ and $G''$ cross-over in the melt state PS(x) ($CaCO_3$/MAA = x); PS (0.0): ▼ $G'$ and ▽ $G''$, PS (0.7): ▲ $G'$ and △ $G''$, PS (0.8): ♦ $G'$ and ◊ $G''$, PS (1.2): ■ $G'$ and □ $G''$, PS (1.4): ● $G'$ and ○ $G''$.

properties in the samples. Indeed, $G''$ becomes higher than $G'$, and the material shows viscous properties.

In the case of the PS(0.0) sample (un-added copolymer), the cross-over temperature is much higher than a pure PS (ca. 150°C). This evolution is the result of the formation of the hydrogen bonds between acid pendant functions, which rises the cross-over temperature.

The presence of the cross-over temperature and the viscous flow zone is a sign of a thermoplastic material. The ionic network in the matrix is then broken. As these rheological analyses are the same when several cooling and warming ramps are applied, the reversibility of the supramolecular network created is ensured.

To conclude, rheological analyses tend to prove the formation of an ionic network and a cluster organization by showing a second transition temperature, called in literature "cluster temperature". They lead to the conclusion that the more the ionic material there is in the matrix, the stronger the ionic bonding inside the multiplet is. Also, they prove the reversibility of the created supramolecular network.

## CONCLUSIONS

This study describes an investigation of the effects of the ionic and filler ratios in an ionic copolymer. Many copolymers of

**Table V.** Temperatures of $G'$ and $G''$ Cross-over in the Melt State

| x ($CaCO_3$/MAA ratio) | Cross-over temperature (°C) |
|---|---|
| 0.0 | 210 |
| 0.7 | 187 |
| 0.8 | 211 |
| 1.2 | 216 |
| 1.4 | - |

poly(styrene-co-methacrylic acid) added with calcium carbonate have been made for the NMR analysis, and the good dispersion in the main chain of the acid functions is proved. The first solubility tests permit us to study the effect of MAA/Sty ([mol]/[mol]) and $CaCO_3$/MAA ([mol]/[mol]) ratios on the formation of an ionic network. Then, the MAA/Sty ([mol]/[mol]) is set to 0.25, and the influence of the calcium-carbonate content has been investigated. The x-ray analysis proved that an ionic supramolecular network is present at every filler content tested, and the study of the filler dispersion ensures that a filling effect is still expected in the matrix.

The rheological analyses allow characterizing the strength of the ionic bonding. The glass transition temperature ("cluster $T_g$") rises with the filler content. Even if the glassy and ionic plateaus do not seem to evolve with the filler content, the rubbery plateau shows an interesting evolution : the tan($\delta$) values increase when the ratio $CaCO_3$/MAA ([mol]/[mol]) decreases, which permits us to conclude that a high density of effective ionic cross-links in the matrix influence the final properties of the material. This conclusion is reinforced by the increase of the loss and storage modulus cross-over temperature, which arises with the calcium content. These analyses show that a hydrogen-bonding network is present in the matrix (seen especially in the case of the non-filled copolymer). Also, they prove the reversibility of the created network as these rheological analyses are the same when several cooling and warming ramps are applied.

The obtained material is a very complicated mixing of several phenomena because the copolymer is not entirely neutralized and not purified and because the calcium carbonate is directly added in the initial monomers' mixtures. There are the calcium-carbonate aggregates and their exfoliation, the ionic organization, and the hydrogen-bonded network to take in account in the final properties. The interest of such a complicated approach due to the wide range of observed phenomena in the material is a one-batch process to make reversible networks.

## ACKNOWLEDGMENTS

This work was supported by the project VALEEE (VALorisation des dEEE) in the cluster AXELERA devoted to the development of new ways in the recycling of polymer from waste of electronic and electric equipments.

## REFERENCES

1. Eisenberg, A.; Kim, J.-S. Introduction to Ionomers, 1st ed.; Wiley-Interscience, New York, **1998**.
2. Schlick, S. Ionomers: Characterization, Theory, and Applications, 1st ed.; CRC-Press, Boca Raton, FL, **1996**.
3. Tant, M. R.; Mauritz, K. A.; Wilkes, G. L. Ionomers: Synthesis, Structure, Properties and Applications, 1st ed.; Springer, Chapman and Hall, London, **1997**.
4. Eisenberg, A.; Hird, B.; Moore, R. B. *Macromolecules* **1990**, *23*, 4098.
5. Yarusso, D. J.; Cooper, S. L. *Macromolecules* **1983**, *16*, 1871.
6. Macknight, W. J.; Taggart, W. P.; Stein, R. S. J. Polym. *Sci. Polym. Symp.* **2007**, *45*, 113.
7. Kim, J.-S.; Jackman, R. J.; Eisenberg, A. *Macromolecules* **1994**, *27*, 2789.
8. Lehn, J.-M. *Rep. Prog. Phys.* **2004**, *67*, 249.
9. Lehn, J. Aust. J. *Chem.* **2010**, *63*, 611.
10. Storey, R. F.; Chisholm, B. J.; Lee, Y. Polym. *Eng. Sci.* **1997**, *37*, 73.
11. Song, J.-M.; Oh, S.-H.; Kim, J.-S.; Kim, W.-G. *Polymer* **2005**, *46*, 12393.
12. Hird, B.; Eisenberg, A. *Macromolecules* **1992**, *25*, 6466.
13. Gauthier, S.; Duchesne, D.; Eisenberg, A. *Macromolecules* **1987**, *20*, 753.
14. Gauthier, M.; Eisenberg, A. *Macromolecules* **1990**, *23*, 2066.
15. Fan, X. D.; Bazuin, C. G. *Macromolecules* **1993**, *26*, 2508.
16. Kim, J. S.; Wu, G.; Eisenberg, A. *Macromolecules* **1994**, *27*, 814.
17. Kim, J.-S.; Hong, M.-C.; Nah, Y. H. *Macromolecules* **2002**, *35*, 155.
18. Castagna, A. M.; Wang, W.; Winey, K. I.; Runt, J. *Macromolecules* **2011**, *44*, 5420.
19. Hirasawa, E.; Yamamoto, Y.; Tadano, K.; Yano, S. J. *Appl. Polym. Sci.* **2003**, *42*, 351.
20. Kim, S.-H.; Kim, J.-S. *Macromolecules* **2003**, *36*, 2382.
21. Luqman, M.; Song, J.-M.; Kim, J.-S.; Kwon, Y. J.; Jarng, S.-S.; Shin, K. *Polymer* **2008**, *49*, 1871.
22. Agarwal, P. K.; Makowski, H. S.; Lundberg, R. D. *Macromolecules* **1980**, *13*, 1679.
23. Tong, X.; Bazuin, C. G. *Chem. Mater.* **1992**, *4*, 370.
24. Kim, J. S.; Roberts, S. B.; Eisenberg, A.; Moore, R. B. *Macromolecules* **1993**, *26*, 5256.
25. Plante, M.; Bazuin, C. G.; Jerome, R. *Macromolecules* **1995**, *28*, 5240.
26. Jackson, D. A.; Koberstein, J. T.; Weiss, R. A. J. Polym. *Sci. Part B: Polym. Phys.* **1999**, *37*, 3141.
27. Kim, J. S.; Shin, K. J.; Kim, D. C.; Kang, Y. K.; Kim, D. J.; Yoo, K. H.; Park, S. W. ChemInform **2003**, 34, 12, doi: 10.1002/chin.200312147.
28. Datta, S.; Bhattacharya, A. K.; De, S. K.; Kontos, E. G.; Wefer, J. M. *Polymer* **1996**, *37*, 2581.
29. Gao, Y.; Choudhury, N. R.; Dutta, N. K. J. *Appl. Polym. Sci.* **2010**, *117*, 3395.
30. Parent, J. S.; Liskova, A.; Resendes, R. *Polymer* **2004**, *45*, 8091.
31. Zhang, W.; Li, M. K. S.; Yue, P.-L.; Gao, P. *Langmuir* **2008**, *24*, 2663.
32. Santamaría, P.; Eguiazábal, J. I.; Nazábal, J. J. *Appl. Polym. Sci.* **2010**, *116*, 2374.
33. Ardanuy, M.; Velasco, J. I.; Rodriguez-Perez, M. A.; Saja, D.; A, J. J. *Appl. Polym. Sci.* **2010**, *116*, 2573.
34. Fraile, J. M.; Garcia, J. I.; Harmer, M. A.; Herrerias, C. I.; Mayoral, J. A.; Reiser, O.; Werner, H. J. Mater. *Chem.* **2002**, *12*, 3290.

35. Colonna, M.; Berti, C.; Binassi, E.; Fiorini, M.; Karanam, S.; Brunelle, D. J. *Eur. Polym. J.* **2010**, *46*, 918.
36. Kiehl, J.; Delaite, C.; Bistac, S.; Schuller, A. S.; Farge, H. *Polymer* **2012**, *53*, 694.
37. Miao, S. *Appl. Surf. Sci.* **2003**, *220*, 298.
38. Shui, M. *Appl. Surf. Sci.* **2003**, *220*, 359.
39. Fekete, E.; Pukánszky, B.; Tóth, A.; Bertóti, I. J. Colloid Interface Sci. **1990**, *135*, 200.
40. Brar, A. S.; Hekmatyar, S. K. J. *Appl. Polym. Sci.* **2001**, *82*, 2444.
41. Fox, T.G. *Bull. Am. Phys. Soc.* **1956**, *1*, 123.